# A $\mu$-Analysis Application to Stability of Optical Networks *

Lacra Pavel
Department of Electrical and Computer Engineering
University of Toronto, 10 King's College Rd, Toronto, ON, Canada, M5S 3G4
pavel@control.toronto.edu

**Abstract** This paper presents an application of control theory and $\mu$-analysis to stability analysis of optical communication networks. The network transfer matrix representation is used and simplified so that the propagation time-delay is isolated on a link-by-link basis. The optical network stability problem is reformulated as a robust stability problem. Sufficient stability conditions are developed by applying $\mu$- analysis and Pade approximation.

## 1 Introduction

Optical communications networks are very recent examples of complex systems that have appeared in the industrial application area of control theory. The evolution from *point-to-point, static* optical links to *mesh, reconfigurable* optical networks (Figure 1), leads to the need to study these systems in a dynamic context, [1]Reconfigurable optical networks are complex systems that encompass tens of dynamic optical devices and distributed propagation time-delays. Since channel routes can be changed dynamically, closed or quasi closed-cycles affected by time-delay can be formed, [2].

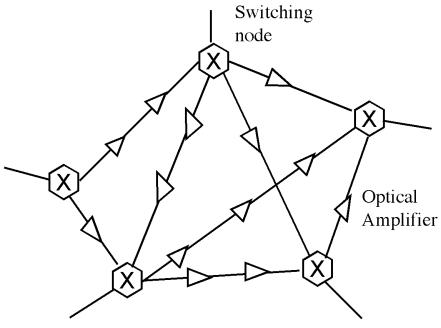


Figure 1: Optical communication network - mesh

Dynamics, stability and control in optical networks are becoming important problems to be addressed, and represent fertile new areas of application of system and control theory.

*This work was supported by the Natural Sciences and Engineering Research Council of Canada

Most existent results at the optical network level are based on extensive simulation or experimental studies of physical networks, followed by development of heuristic rules. Recent studies, [7], [8], [9], have shown that for a generic network configuration as in Figure 2, transient dynamical behaviour is observed. At reconfiguration or at failures, sudden power changes on some channels can cause abrupt power changes on other channels, followed by transient fluctuations. In some cases these fluctuations lead even to a sustained oscillation regime in the network, or instability. This behavior was observed in simulations and experiments only, and based on this, heuristic rules developed for avoiding it. However, there are no rigorous analysis approaches developed to address this problem. These observations highlight the need for a theoretical understanding of optical network dynamics and stability.

In this paper we address the network stability problem for a generic configuration as in Figure 2. We use the modeling framework proposed in [10], where a more comprehensive treatment of this problem is given. We find sufficient conditions for network stability based on application of $\mu$-analysis. We relate them to the sustained oscillations regime, previously observed by means of simulation and experiments. These results can be used in reconfigurable networks, where routing algorithms could decide whether or not to configure an optical path based on a preliminary stability analysis.

In Section 2 we formulate the problem for a generic optical network configuration, and review the results on optical network modeling. In Section 3 we address network stability by reformulating it as a robust stability problem. We use the Pade approximation for the path propagation time-delays, and we resort to $\mu$-analysis. Simulation results are shown in Section 4 and conclusions in Section 5.

## 2 Optical Network Modeling

A network configuration typically used in the communication industry is shown in Figure 2. This configuration is representative for a quasi-ring optical path, [2], that can be extracted from a mesh topology (Figure 1).

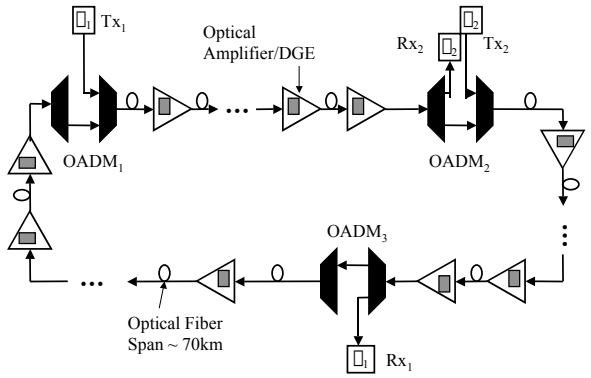


Figure 2: Optical communication network: quasi-ring

Multiple optical signals, corresponding to channels at different wavelengths (optical frequencies), are transmitted together on a single optical fiber, resulting in a wavelength-division multiplexed (WDM) system. Optical amplifiers (OA) in combination with dynamic gain equalizers (DGE) are used every few tens of km to compensate the power loss that occurs during light propagation through the optical fiber. Optical add-drop multiplexers (OADM), are used to separate and recombine wavelength channels or for switching. OADM constitute network nodes. Each optical communication link between two adjacent OADM nodes is composed of several cascaded optically amplified spans.

Let $u$ and $y$ denote the network input and output optical power vectors in Figure 2, partitioned as

$$u = \left[ \begin{array}{c} u_1 \\ u_2 \end{array} \right], \; y = \left[ \begin{array}{c} y_1 \\ y_2 \end{array} \right], \; u_{1,2}, y_{1,2} \in R^{m_{1,2}} \qquad (1)$$

corresponding to the two wavelength sets, $\lambda_1$ and $\lambda_2$, each with $m_1$ and $m_2$ channels, $m = m_1 + m_2$.

$$\lambda_1 = \left\{ \; \lambda_{1,1}, ...\lambda_{1,m_1} \; \right\}, \; \lambda_2 = \left\{ \; \lambda_{2,1}, ...\lambda_{2,m_2} \; \right\} \quad (2)$$

Channels $\lambda_1$ are added (transmitted) at the $\mathrm{Tx}_1$ site ($\mathrm{OADM}_1$) and dropped (received) at the $\mathrm{Rx}_1$ site ($\mathrm{OADM}_3$). Channels $\lambda_2$ are added at the $\mathrm{Tx}_2$ site ($\mathrm{OADM}_2$) and dropped at the $\mathrm{Rx}_2$ site ($\mathrm{OADM}_2$).

For a general LTI system with transfer matrix $G(s)$, $y = G(s)u$, we define the related system, $\widetilde{G}$, that maps $u$, (1), to the reversed output vector, $\widetilde{y} \in R^{(m_2+m_1)}$

$$\widetilde{y} = \widetilde{G}u, \quad \widetilde{y} = \left[ \begin{array}{c} y_2 \\ y_1 \end{array} \right], \quad \widetilde{G} = \left[ \begin{array}{cc} 0 & I_{m_2} \\ I_{m_1} & 0 \end{array} \right] G \quad (3)$$

In the following we review the results in [10] on optical network modeling. The approach involves firstly developing transfer matrix models for individual network elements, optical spans and optical links. Then the optical network model is developed using interconnections rules and linear fractional transformation (LFT) techniques. The closed-form transfer matrix can be used to study network dynamics and transient response.

Through an optical fiber, signals experience loss and propagation time-delay. The fiber loss coefficient, which is typically the same for all channels, can be incorporated into the amplifiers model. For propagation time-delay we will use the following assumption.

**(A1):** In a WDM network, all channels in an optical span (link) experience essentially the same propagation time-delay.

This assumption is justified as follows. In an optical span, different channels (wavelengths) are sharing the same optical fiber. For typical span lengths of tens of kilometers, the average propagation induced delay for all channels is on the order of fractions of $ms$. Due to modal dispersion, [3], different channels (wavelengths) will travel with slightly different speeds. Hence, due to dispersion, they will experience slightly different delays, called dispersion induced delays. However, in an optical system, , for adequate receiver detection, dispersion management techniques are used periodically, [3]. As a result, dispersion induced delay (pulse broadening) is maintained at a fraction of the bit period, i.e., typically fractions of $nsec$. Therefore, at the end of an optical span (link), the dispersion induced delay difference between channels is considerable smaller than the average propagation induced delay. This shows that, at least on network reconfiguration time-scales, i..e, from $\mu$s to hundreds of ms, assumption (A1) is valid.

Therefore the following relation holds in the frequency domain across an optical fiber span

$$y_s(s) = \alpha \, \mathcal{D}_\tau(s) u_s(s) \qquad (4)$$

$$\mathcal{D}_\tau(s) = e^{-\tau s} I_m \qquad (5)$$

with $\alpha$ being the scalar fiber loss coefficient and $\tau$ the propagation time-delay across a span, respectively.

An optically amplified span consists of an optical fiber and an optical dynamic amplifier (ODA) (optical amplifier /DGE blocks in Figure 2). An ODA is realized by combining optical amplifiers, $G_{OA}$, with DGEs. An optical amplifier has active control for maintaining total output power or total gain constant. For Erbium-doped fiber optical amplifiers, typically used, a linearized model $G_{OA}$, is a MIMO, square transfer matrix, [4], [6]. Diagonal terms have a high-pass behavior, and off-diagonal terms have a low-pass behavior, with typical time-constants on the order of 1 - 10 ms. These are comparable to network reconfiguration time-scales, and hence affect cross-coupling dynamics between groups of wavelengths.

DGEs have spectrally adjustable attenuation, and are used for equalizing wavelength channel powers, [5], [6]. A linearized model of the ODA, $G_{ODA}$, can be developed, [10], as a feedback interconnection of $G_{OA}$ with a MIMO ($m$ x $m$) diagonal controller, $K_{DGE}(s)$,

$$G_{ODA}(s) = G_{OA}(s)(I_m + K_{DGE}(s)G_{OA}(s))^{-1} \quad (6)$$

$$K_{DGE}(s) = \begin{bmatrix} K_1(s) & \cdots & 0 \\ & \ddots & \\ 0 & \cdots & K_m(s) \end{bmatrix}$$

Let the $k^{th}$ optical span be described by a MIMO transfer matrix, $G_{(k)}(s)$, that combines the transfer matrix of ODA, $G_{ODA}(s)$, and loss of optical fiber, $\alpha$. Including the delay effects, the span overall transfer matrix, $G_{\mathcal{D},(k)}(s)$, is given as

$$G_{\mathcal{D},(k)}(s) = G_{(k)}(s)\mathcal{D}_\tau(s) \quad (7)$$

where $\mathcal{D}_\tau(s)$ is defined in (5). An optical link has the transfer matrix given next.

**Lemma 1 :** *The transfer matrix of an optical communication link, $S_{\mathcal{D}}(s)$, realized by a series interconnection of $N$ optical spans is given as*

$$S_{\mathcal{D}}(s) = \mathcal{D}_N(s)S(s) = S(s)\mathcal{D}_N(s)$$

$$S(s) = \prod_{k=1}^{N} G_{(k)}(s), \quad \mathcal{D}_N(s) = e^{-(N\tau)s} I_m$$

*where $G_{(k)}(s)$, (7), is the span transfer matrix, and $\tau$ is the span time-delay.*

**Proof:** [10]. ■

The following result gives the transfer matrix of the optical network in Figure 2. Let $P_{\mathcal{D}}$, $Q_{\mathcal{D}}$ and $X_{\mathcal{D}}$ denote the optical link transfer matrices for Figure 2, given as in Lemma 1. Recall that $u$ and $y$, (1), denote the network input and output optical power vectors, partitioned accordingly to the two wavelength sets, $\lambda_1$ and $\lambda_2$, (2). Then the equivalent network block diagram for Figure 2 is shown in Figure 3.

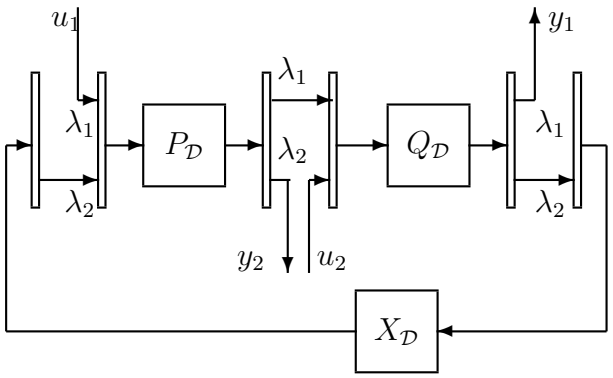


Figure 3: Network: Block-Diagram

**Theorem 2 :** *The transfer matrix, $\mathcal{T}$, of the optical communication network in Figure 2 (or Figure 3)*

$$\begin{bmatrix} y_1 \\ y_2 \end{bmatrix} = \mathcal{T} \begin{bmatrix} u_1 \\ u_2 \end{bmatrix}, \mathcal{T} = \begin{bmatrix} \mathcal{T}_{11} & \mathcal{T}_{12} \\ \mathcal{T}_{21} & \mathcal{T}_{22} \end{bmatrix}$$

*is given as (Figure 4)*

$$\mathcal{T} = \begin{bmatrix} 0 & I_{m_1} \\ I_{m_2} & 0 \end{bmatrix} \Re\left( \widetilde{P}_{\mathcal{D}}, \begin{bmatrix} X_{\mathcal{D}} & 0 \\ 0 & I_{m_2} \end{bmatrix} \widetilde{Q}_{\mathcal{D}} \right) \quad (8)$$

*where $\Re(\cdot,\cdot)$ is the Redheffer star-product, [11], and $\widetilde{P}_{\mathcal{D}}$, $\widetilde{Q}_{\mathcal{D}}$, and $X_{\mathcal{D}}$ are related to the optical link transfer matrices, $P_{\mathcal{D}}$, $Q_{\mathcal{D}}$ and $X_{\mathcal{D}}$, as in (3).*

*For partitions according to the two wavelength sets*

$$P_{\mathcal{D}} = \begin{bmatrix} P_{\mathcal{D},11} & P_{\mathcal{D},12} \\ P_{\mathcal{D},21} & P_{\mathcal{D},22} \end{bmatrix}, \; Q_{\mathcal{D}} = \begin{bmatrix} Q_{\mathcal{D},11} & Q_{\mathcal{D},12} \\ Q_{\mathcal{D},21} & Q_{\mathcal{D},22} \end{bmatrix}$$

*the transfer matrix $\mathcal{T}$ has partitions $\mathcal{T}_{ij}$, $i,j = 1,2$,*

$$\begin{aligned} \mathcal{T}_{11} &= Q_{\mathcal{D},11}\, \Psi_{\mathcal{D}} P_{\mathcal{D},11} \\ \mathcal{T}_{12} &= Q_{\mathcal{D},12} + Q_{\mathcal{D},11}\, P_{\mathcal{D},12}\, \widetilde{\Psi}_{\mathcal{D}}\, X_{\mathcal{D}}\, Q_{\mathcal{D},22} \\ \mathcal{T}_{21} &= P_{\mathcal{D},21} + P_{\mathcal{D},22}\, X_{\mathcal{D}}\, Q_{\mathcal{D},21}\, \Psi_{\mathcal{D}}\, P_{\mathcal{D},11} \\ \mathcal{T}_{22} &= P_{\mathcal{D},22}\, \widetilde{\Psi}_{\mathcal{D}} X_{\mathcal{D}}\, Q_{\mathcal{D},22} \end{aligned} \quad (9)$$

*where*

$$\begin{aligned} \Psi_{\mathcal{D}} &= \left( I - P_{\mathcal{D},12}\, X_{\mathcal{D}}\, Q_{\mathcal{D},21} \right)^{-1} \\ \widetilde{\Psi}_{\mathcal{D}} &= \left( I - X_{\mathcal{D}}\, Q_{\mathcal{D},21}\, P_{\mathcal{D},12} \right)^{-1} \end{aligned} \quad (10)$$

**Proof:** [10]. ■

As seen from Theorem 2 and Figure 4, explicit cross-coupling exists between group 1 and 2 of channels, as given by $\mathcal{T}_{12}$, $\mathcal{T}_{21}$. These transfer matrices are directly dependent on the time-delay link transfer matrices, $P_{\mathcal{D}}$, $Q_{\mathcal{D}}$, $X_{\mathcal{D}}$, as well as on the feedback terms, $\Psi_{\mathcal{D}}$, $\widetilde{\Psi}_{\mathcal{D}}$.

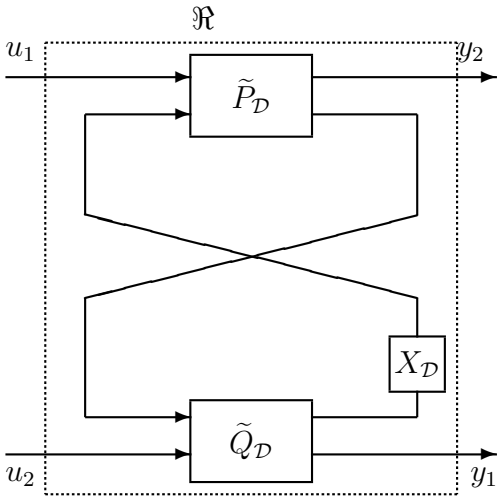


Figure 4: Network: Star-Product Representation

## 3 Network Stability by $\mu$-Analysis

In the following we use these results to address the network stability problem. Using (A1) we will show that the distributed propagation time-delays can be lumped on a link-by-link basis, and isolated as a delay block on a path-by-path basis.

**Theorem 3 :** *Under (A1), the optical network (Figure 2, or Figure 3) is stable if and only if the feedback loop configuration in Figure 5 (b) is stable, where $L$ is the loop transfer matrix that describes the cross-coupling, and $\mathcal{D}_t$ is the total path delay-block*

$$L = P_{12}\, X\, Q_{21} \quad \mathcal{D}_t = e^{-\tau_t s}\, I_{m_1} \tag{11}$$

*and $\tau_t = (N_1 + N_2 + N_3)\,\tau$ is the total network propagation delay.*

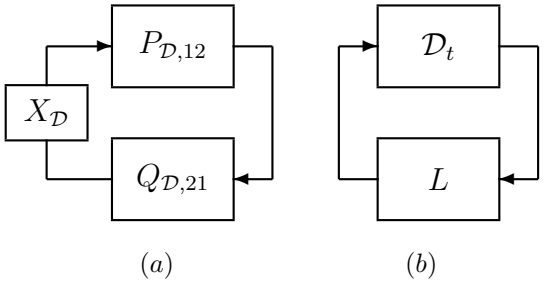


Figure 5: Network Stability: Loop Configuration

**Proof:** Recall (9) where, from Lemma 1, the optical links $P_{\mathcal{D}}$, $Q_{\mathcal{D}}$ and $X_{\mathcal{D}}$ are given as

$$\begin{aligned} P_{\mathcal{D}}(s) &= \mathcal{D}_{N_1}(s)P(s), \quad P(s) = \textstyle\prod_{k=1}^{N_1} G_{(k)}(s) \\ Q_{\mathcal{D}}(s) &= \mathcal{D}_{N_2}(s)Q(s) \quad Q(s) = \textstyle\prod_{k=1}^{N_2} G_{(k)}(s) \\ X_{\mathcal{D}}(s) &= \mathcal{D}_{N_3}(s)X(s) \quad X(s) = \textstyle\prod_{k=1}^{N_3} G_{(k),22}(s) \end{aligned} \tag{12}$$

with

$$\mathcal{D}_{N_i}(s) = e^{-(N_i\tau)s} I_m$$

denoting the delay-terms on a link-by-link basis, for $N_1, N_2$ and $N_3$ optical fiber spans, respectively. Therefore, as cascades of stable systems, optical links $P_{\mathcal{D}}$, $Q_{\mathcal{D}}$ and $X_{\mathcal{D}}$ and their partitions in (9) are also stable.

From (9)and Figure 4 it follows immediately that internal stability of the optical network is equivalent to stability of the system $\Psi_{\mathcal{D}}$, or equivalently $\widetilde{\Psi}_{\mathcal{D}}$, (10). From the definition of $\Psi_{\mathcal{D}}$, (10), we see that stability of the feedback system $\Psi_{\mathcal{D}}$ can be found by representing it in a feedback loop configuration as in Figure 5 (a).

Note that in Figure 5 (a), link time-delay blocks $\mathcal{D}_{N_i}(s)$ are distributed across the path, as given in (12). However, by (A1) all channels in an optical link experience the same propagation delay. Based on this, simple manipulations can be used to show how the link time-delay blocks can lumped together in a single optical path delay-block. For example, for the partition $P_{\mathcal{D},12}$ as in (12), we can write

$$P_{\mathcal{D},12} = e^{-(N_1\tau)s}\, P_{12}(s) = P_{12}(s)\, e^{-(N_1\tau)s}$$

Proceeding similarly for the other factors in (10), we get

$$\Psi_{\mathcal{D}} = \left(\; I - P_{12}(s)\, X(s)\, Q_{21}(s)\, e^{-\tau_t s}\, I_{m_1} \;\right)^{-1}$$

where $\tau_t = (N_1 + N_2 + N_3)\,\tau$ is the path delay.

Equivalently, using (11),

$$\Psi_{\mathcal{D}} = \left(\; I - L(s)\; \mathcal{D}_t(s) \;\right)^{-1}$$

where $\mathcal{D}_t = e^{-\tau_t s}\, I_{m_1}$ is a single path total delay-block.

Then, stability of $\Psi_{\mathcal{D}}$, and hence of the network, is equivalent to stability of the feedback configuration in Figure 5 (b). ■

**Remark:** Note that for typical transfer matrices, by applying the small gain theorem, stability of the feedback system in Figure 5 (b) could be analyzed in terms of the $H_\infty$ norm of the loop transfer matrix. As seen from (11), the presence of the time-delay block $\mathcal{D}_t$ on the feedback path of the MIMO loop transfer matrix $L$ precludes the direct application of such a result.

We will use the approach in [13], based on the Padé approximation technique, and the use of robust stability and $\mu$-analysis.

Recent studies on the quality of the Padé approximation in $H_\infty$ and $L_1$ norm sense, and on the order of the rational approximation for a delay bandwidth of a given system, were done in [14] and [15], respectively. Padé approximations are appropriate to use particularly for low bandwidths. We are concerned here with low loop time-delay bandwidths, on similar time-scales as network reconfiguration time-scale. These are on the order of $ms$, i.e., on much slower time-scales than the fast bit periods ($nsec$), so that the use of a low order Padé approximation is justified.

Then the following network stability result is given.

**Theorem 4 :** *Under (A1), stability of the optical network in Figure 2 (or Figure 3) is equivalent to robust stability of the closed loop system in Figure 6 (b), where*

$$M(s) = F_l(\mathbf{G}_{\mathbf{x},\mathbf{Pade}}(s), L(s)) \tag{13}$$

*is assumed stable, with $L(s)$ being the loop transfer matrix, (11), and $\mathbf{G}_{\mathbf{x},\mathbf{Pade}}(s)$ the known LFT system for the uncertain Padé approximation of $\mathcal{D}_t$, (11). Therefore, the closed-loop system is stable if and only if*

$$\sup_{\omega} \mu_{\Delta}(M(j\omega)) < \beta \quad \forall w \tag{14}$$

*for all* $\mathbf{\Delta}$ *such that*

$$\| \mathbf{\Delta} \|_\infty \leq \frac{1}{\beta}, \quad \| \mathbf{\Delta}(s) \|_\infty = \max_\omega \bar{\sigma}(\mathbf{\Delta}(j\omega))$$

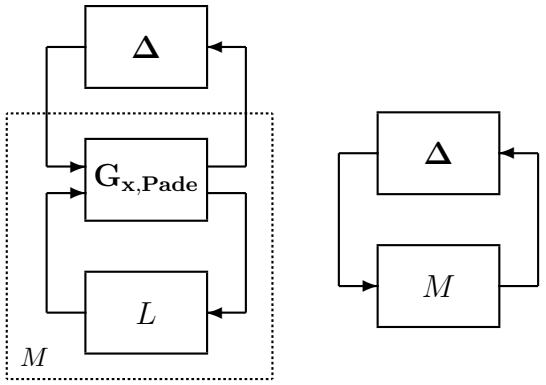


(a) (b)

Figure 6: Network Stability: MΔ Configuration

**Proof:**

Let the delay $\tau_t$ be expressed as

$$\tau_t = \tau_0 + \delta_0 \, \Delta, \quad \Delta \in [-1, 1]$$

with $\tau_0$ some nominal delay, $\delta_0$ a known scalar, and $\Delta$ an unknown but bounded real scalar ($-1 \leq \Delta \leq 1$).

Let a single-channel delay $e^{-\tau_t s}$ be approximated by a $1^{st}$ order Padé LTI system

$$e^{-\tau_t s} \approx \frac{1 - \frac{\tau_t}{2} s}{1 + \frac{\tau_t}{2} s} = 1 - \left( \; 1 + \frac{\tau_t}{2} s \; \right)^{-1} \tau_t s$$

Then an upper linear fractional representation (LFT) of the $1^{st}$ order Padé approximation is given as

$$\frac{1 - \frac{\tau_t}{2} s}{1 + \frac{\tau_t}{2} s} = F_u(G_{x,Pade}(s), \Delta) \tag{15}$$

where

$$G_{x,Pade}(s) = \begin{bmatrix} -\frac{\frac{\delta_0}{2} s}{1 + \frac{\tau_0}{2} s} & \frac{2s}{1 + \frac{\tau_0}{2} s} \\ -\frac{\frac{\delta_0}{2}}{1 + \frac{\tau_0}{2} s} & \frac{1 - \frac{\tau_0}{2} s}{1 + \frac{\tau_0}{2} s} \end{bmatrix}$$

and $\Delta \in [-1, 1]$. In state-space form $G_{x,Pade}(s) = (A_x, B_x, C_x, D_x)$ with

$$A_x = -\frac{2}{\tau_0} \qquad B_x = \begin{bmatrix} -\frac{\delta_0}{\tau_0} & \frac{4}{\tau_0} \end{bmatrix}$$

$$C_x = \begin{bmatrix} -\frac{2}{\tau_0} \\ 1 \end{bmatrix} \qquad D_x = \begin{bmatrix} -\frac{\delta_0}{\tau_0} & \frac{4}{\tau_0} \\ 0 & -1 \end{bmatrix}$$

Now, extending (15) to the multichannel delay, $\mathcal{D}_t(s)$, (11), (Figure 5 (b)), we have

$$\mathcal{D}_t(s) = e^{-\tau_t s} \, I_{m_1} \approx F_u(\mathbf{G_{x,Pade}}(s), \mathbf{\Delta}) \tag{16}$$

where $\mathbf{\Delta} = \Delta * I_{m_1}, \quad \Delta \in [-1, 1]$

and $\mathbf{G_{x,Pade}}(s)$ is a ($m_1$ x $m_1$) diagonal system

$$\mathbf{G_{x,Pade}}(s) = \begin{bmatrix} G_{x,Pade}(s) & \cdots & 0 \\ & \ddots & \\ 0 & \cdots & G_{x,Pade}(s) \end{bmatrix}$$

Then using (16), we see that configuration in Figure 5 (b) is equivalent to Figure 6 (a), and the result follows from standard small gain theorem and $\mu$-analysis theory, [12], [11]. The basic idea is to rearrange the system (Figure 6 (a)) in a $M\Delta$ structure (Figure 6 (b)), where $M$ is given as

$$M(s) = F_l(\mathbf{G_{x,Pade}}(s), L(s))$$

and represents the transfer matrix from the output to the input of the perturbation. Then use of the robust stability condition (14) ensures stability. ■

**Remark:** Notice that this robust stability problem is in the class of repeated real diagonal perturbations, since the uncertainty in each channel is identical. The calculated $\mu$ value gives the magnitude of the tolerated perturbation before getting to instability. A particular $\mathbf{\Delta}$ that will cause instability can be found such that

$$\| \mathbf{\Delta} \|_\infty \leq \frac{1}{\beta_l}$$

where $\beta_l$ is the peak of the lower bound of the $\mu$-value, [12]. This gives the maximum delay $\overline{\tau}$, or maximum path length before instability,

$$\overline{\tau} = \tau_0 + \delta_0 \, \frac{1}{\beta_l}$$

## 4 Simulation results

As an example we consider the problem of network reconfiguration with varying path length. The nominal network in Figure 2 has twelve optical dynamic amplifier spans, (7), each span of a length of approximately 70 km, corresponding to $\tau \approx 0.33$ ms delay. There are 80 wavelength channels grouped in 10 sub-bands propagating across a total 12 x 70 km loop, with a nominal total delay of $\tau_0 \approx 4$ ms. We assume that the two groups $\lambda_1$ and $\lambda_2$ are equal. We will use the results in Theorem 4 to get a measure of the maximum path length (total delay) that could be used at network reconfiguration. Numerical calculation using the $\mu$ toolbox (Matlab) gives $\mu = 1.05$, yielding a destabilizing perturbation of $\overline{\tau_t} \approx 15$ ms.

We simulate network reconfiguration by a sudden increase in power on the $\lambda_2$ group. Results are shown for

varying loop time-delay (loop path length). As seen in Figure 7 (a), for nominal delay, both groups of wavelengths experience power fluctuations until settled. For the case when the loop path and time-delay is four times larger, $\overline{\tau_t} \approx 16$ ms, the network becomes unstable, with sustained oscillations. This shows that the results of Theorem 4 provide a good estimate although slightly conservative. Also, they correspond to the simulation and experimental results of physical networks, [8], [9].

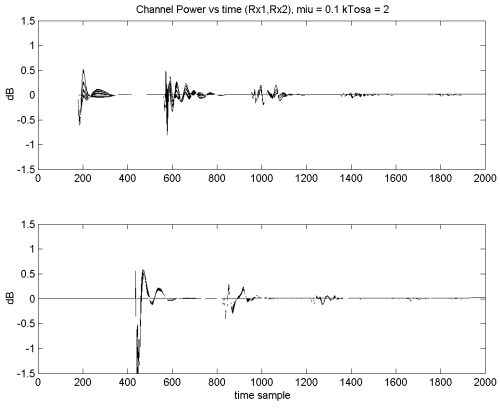


(a)

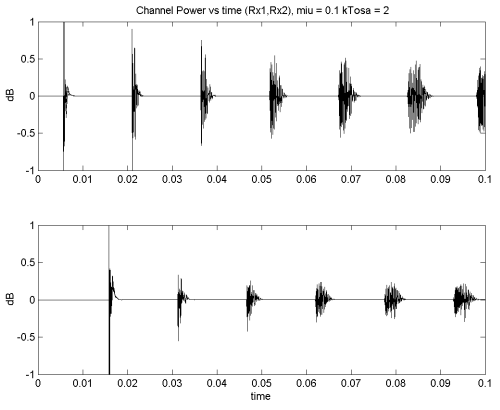


(b)

Figure 7: Simulation results: (a) nominal time-delay (optical path length), (b) four times larger

## 5 Conclusions

This paper presented an application of control theory and $\mu$-analysis to stability analysis in optical communications networks. A generic network configuration was considered. The transfer matrix representation evidences coupling on the feedback path between two channel groups as well as propagation time-delay.

The network stability problem was reformulated as a robust stability problem. We used a Pade approximation for the overall path delay, suitable for the low frequencies used for network reconfiguration (as compared to the high data rates). We applied $\mu$-analysis to derive sufficient conditions for network stability. Future work will extend these conditions, such that explicit dependence on network parameters can be evidenced.

## References


[1] Mukherjee, B.,'WDM optical communication networks: progress and challenges', *IEEE J. Selected Areas Commun.*, vol. **18**, 1810-1824, 2000.

[2] Bala, K., C.A. Brackett, 'Cycles in wavelength routed optical communication networks', *J. Lightwave Technol.*, vol. **14**, 1585-1594, 1996.

[3] Agrawal, G.P., *Fiber-optic communication systems*, Wiley-Interscience, John Wiley, 2002.

[4] Sun, Y., J. L. Zyskind, A. K. Srivastava, 'Average inversion level, modeling, and physics of Erbium-doped fiber amplifiers', *IEEE J. Sel. Topics in Quantum Electronics*, vol. **3**, 991-1007, 1997.

[5] Ford, J.E., J.A. Walker,'Dynamic spectral power equalization using micro-optomechanics',*IEEE Phot. Tech. Letters*, vol. **10**, 1440-1442. 1998.

[6] Pavel, L., 'Control design for transient power and spectral control in optical communication networks', *Proc. IEEE CCA*, 415-422, June 2003.

[7] Yoo, S. J. B., W. Xin, et al., 'Observation of prolonged power transients in a reconfigurable multiwavelength network and their suppression by gain-clamping of optical amplifiers', *IEEE Phot. Tech. Lett.*, vol.**10**, 1659-1661, 1998.

[8] Kim, P., S. Bae, S. J. Ahn, N. Park, 'Analysis on the channel power oscillation in the closed WDM ring network with the channel power equalizer', *IEEE Phot. Tech. Lett*, **12**, 1409-1411, 2000.

[9] Pavel, L., 'Effect of equalization strategy on dynamic response of optical communication networks', *Proc. IEEE LEOS 2002*, 185-186, 2002.

[10] Pavel, L., 'Dynamics and stability in optical communication networks: A system theoretic framework', *under review, Automatica.*

[11] Zhou, K., J.C. Doyle, K. Glover., *Robust and Optimal Control*, Prentice-Hall, 1996.

[12] Packard A, J. Doyle, 'The complex structured singular value', *Automatica*, vol. **29**, 71-109, 1993.

[13] Niculescu, S-I., *Delay Effects on Stability - A Robust Control Approach*, Springer-Verlag, 2001.

[14] Makila, P. M., J. R. Partington, 'Shift operator induced approximations of delay systems', in *SIAM J. Control Optimization*, **37**, 1897-1912, 1999.

[15] Al-Amer, S.H., Al-Sunni, F.M. 'Approximation of time-delay systems', *Proc. ACC*, 1935-1939, 2000.